SPATIAL STRUCTURE IN THE 10 MICRON SPECTRUM OF HD 44179 (THE RED RECTANGLE)[1]

G. L. GRASDALEN

G-Star Enterprises, 286 S. Pennsylvania, Denver, CO 80209

G. C. SLOAN

Department of Physics and Astronomy, University of Wyoming, Laramie, WY 82071

AND

P. D. LEVAN

Phillips Laboratory, Hanscom AFB, MA 01731

ABSTRACT

We present long-slit 10 μm spectra of HD 44179. The object is resolved in the unidentified infrared features at 7.7, 8.6, and 11.3 μm. Another feature at 12.8 μm, which may be related to the unidentified infrared features or may be [Ne II], is similarly resolved. The source of the smooth underlying continuum is only marginally resolved by the present observations and analysis. These results demonstrate the power of long-slit spectra in revealing spatial structures via their spectral signature.

Subject headings: infrared: stars — stars: individual (HD 44179)

1. INTRODUCTION

Cohen et al. (1975) first associated the infrared source GL 915, discovered in the AFGL sky survey (Walker & Price 1975), with the bipolar nebula surrounding HD 44179. Due to its striking rectangular shape on the red Palomar Sky Survey plates, they named the object the Red Rectangle. The central star, HD 44179, has a spectral type of B9-A0 IIIe. The Na D and Ca II K lines are in emission, as well as a broad feature centered at 0.69 μm. The optical nebulosity covers $\sim 40''$.

Zuckerman et al. (1976) postulated that HD 44179 is an evolved star, perhaps a proto–planetary nebula, based on its many similarities with the suspected proto–planetary nebulae GL 2688 (the Cygnus Egg; Ney et al. 1975; Crampton, Crowley, & Humphreys 1975) and GL 618 (the Westbrook Nebula; Westbrook et al. 1975). These similarities include the bipolar structure of the visible reflection nebulae and the strong thermal emission from the central regions at mid-infrared wavelengths. None of these objects are associated with any signs of star formation. Additional support for their evolved status comes from the carbon-rich nature of the heated dust and the high galactic latitude of these sources. All exhibit CO emission typical in outflows from evolved stars (Bachiller et al. 1988). The case for the proto–planetary nebula stage is strongest for GL 618, which has a variety of forbidden emission lines along with Balmer emission in its visible spectrum (Westbrook et al. 1975), indicating that UV radiation from the stellar core is beginning to ionize the surrounding material.

HD 44179 is unique among these objects in that its infrared spectrum contains the entire family of unidentified infrared (UIR) emission features at 3.3, 6.2, 7.7, 8.6, and 11.3 μm (Russell, Soifer, & Willner 1978). A variety of materials have been invoked to explain these features, but none are completely adequate (see Sellgren 1990 for a recent review). These materials include polycyclic aromatic hydrocarbons (e.g., Léger & d'Hendecourt 1987), amorphous carbon material (Duley & Williams 1981), quenched carbonaceous composites

(Sakata et al. 1987) and hydrogenated amorphous carbon (Blanco, Bussoletti, & Colangeli 1988). These features have drawn much attention to HD 44179, primarily at 3.3 μm (e.g., Tokunaga & Young 1980; Geballe et al. 1985; Tokunaga et al. 1988; Geballe et al. 1989).

Speckle interferometric methods have resolved the central thermal emission of HD 44179 into two sources at near-infrared wavelengths, a compact source $0''.2$ across and an extended source $1''.0$ N/S by $0''.4$ E/W (Dyck et al. 1984; Dainty et al. 1985; Leinert & Haas 1989). In a study of the UIR features, Geballe et al. (1989) detected 3.3 μm UIR emission $5''$ north of HD 44179, indicating that the region producing this emission is very extended.

It is likely that the UIR features at longer wavelengths are also extended, so we chose to examine the spatial nature of the spectrum of HD 44179 at 10 μm with a slit spectrometer. We have also observed α Ori to serve as a check on our results, since the spatial extent of its emission at 10 μm is fairly well understood (Dyck & Benson 1991).

2. OBSERVATIONS AND DATA REDUCTION

The data were obtained with the Geophysics Laboratory Array Detector Spectrometer (GLADYS) mounted on the University of Wyoming Infrared Observatory's (WIRO) 2.3 m telescope. GLADYS disperses radiation from 7 to 14 μm onto a Si:Ga detector array with a NaCl prism; it is described in more detail by LeVan (1990). GLADYS was controlled by the WIRO computer system, which also collected the data and displayed it during the observations. In all spectra, the entrance slit was kept in a north/south orientation. The secondary mirror was chopped at a frequency of 1.5 Hz with a throw of $23''$ N/S.

Until recently the instrument was plagued by digital difficulties which resulted in repeatable but flawed data. These difficulties were finally overcome in late 1990, and GLADYS performed splendidly during the 1991 February run.

Since the original description of GLADYS a more sensitive array has been installed in the dewar. In the current configuration the same 10 columns of the chip are read 3 times during

a cycle that formerly sampled 29 columns of the array. This procedure avoids the possibility of filling the wells with the larger currents produced by the more sensitive chip, but it also limits the extent of the slit to 9″ on the sky. The new array was installed with the short-wavelength cutoff at 7 μm.

A further innovation has been the implementation of three-beam chopping (Landau, Grasdalen, & Sloan 1992). This technique does not require repositioning the telescope during an integration, so it is far more appropriate for the present experiments, which require the highest possible spatial stability.

Flat fields for the array are obtained by saturating polystyrene foam with liquid nitrogen and then staring at it with GLADYS while it warms to ambient temperatures. As it warms, the flux on each pixel of the array increases. By taking the difference between the frames obtained at the highest and lowest flux levels we obtain very satisfactory flat fields. These flat fields have been verified by further staring observations of the night sky at different zenith distances and chopped observations of Jupiter.

After division by the flat field the data are spline-interpolated to remove the slight misalignments between the slit and dispersion axes and the chip axes. The slit and dispersion axes are physically independent; rotating the images will only remove one of these misalignments. This procedure carries a significant risk of degrading the data, but the effects we report in this *Letter* are well above any threshold for concern.

The last step in the basic data reduction is to correct for spectral transmission of the atmosphere and instrument. This is accomplished by obtaining observations of photometric, point source standard stars. Since columns in the interpolated data array now correspond to a single wavelength, the calibration merely consists of obtaining a spectrum by summing the observed intensities along each column. The flat-fielded images are then divided by spectra of α Tau. Contour maps of the reduced data for α Tau, α Ori, and HD 44179 are shown in the left-hand panels of Figure 1.

3. ANALYSIS

Inspection of the contour maps displayed in Figure 1 leads one to suspect that α Ori and HD 44179 show spatial structure in their spectra. To examine this possibility quantitatively, we fitted the spatial profile in each column (i.e., at each wavelength) with the following function:

$$I = I_n \left\{ \exp\left[\frac{-(x_n - x)^2}{\sigma_n^2} \right] + 0.25 \exp\left(-0.65 \, |x_n - x| \right) \right\},$$

where I_n controls the central intensity in column n, x_n is the interpolated central spatial position in column n, and σ_n is the spatial width for column n. Although we arrived at this form of the profile by empirically fitting the spatial profile we have found that the second term represents reasonably closely the wings of the diffraction profile predicted for the 2.3 m telescope over the 10 μm window. Therefore this term in the profile function *does not* (to first order) scale with the spatial extent of the object.

We have tested this technique by applying it to the observations of α Ori and α Tau. In the right-hand panels of Figure 1 we have plotted the parameter σ obtained by fitting equation (1) to each column of the data. We refer to these plots as spatiograms.

First we discuss the behavior of σ with wavelength for α Tau.

The gradual increase in σ beyond 10 μm is expected on the basis of the increasing size of the diffraction pattern. The behavior shortward of 10 μm is more difficult to analyze. Here the point spread function is most severely undersampled, so that our reduction techniques are less reliable. Further, the ozone absorption feature appears to play a major role in controlling the width and position of the spectrum, because of the changes in refractive index around this strong absorption feature. Similar comments apply to the region shortward of 8 μm, a region of very strong atmospheric absorption.

The behavior of σ with wavelength for α Ori is dramatically different. The excess width in the α Ori spectrum clearly follows the infrared excess for this object, rising abruptly near 9 μm, peaking at $\sim$9.7 μm and falling gradually toward longer wavelengths. This is precisely the behavior that is expected based on the analysis of Dyck & Benson (1991). The present observations go somewhat further in that they clearly identify the spatial extent with the silicate feature. This expected result gives us considerable confidence in our method of analysis.

The HD 44179 data were taken from a 1 hour integration on 1991 February 10, divided into four groups, analyzed separately, and the results combined to form a mean and an estimate of the standard deviation. There are four peaks present in the spatiogram of HD 44179 that are not present in α Tau. The three largest are centered at 7.7, 8.6, and 11.3 μm, the classic UIR features in the 10 μm region. The weakest and apparently narrowest peak occurs at 12.8 μm. This feature may be related to the UIR feature at 11.3 μm (Cohen, Tielens, & Allamandola 1985; Witteborn et al. 1989). From our observations, however, we cannot rule out the possibility that [Ne II] is responsible for the feature. There is marginal evidence that the underlying continuum in HD 44179 is also resolved. The observations of α Tau were obtained immediately before and after the observations of HD 44179. The fact that the spatiogram for HD 44179 follows very closely the results for α Tau in the regions outside of the spectral features means that the size of the central source is not a strong function of wavelength.

In Figure 2 we present the spectrophotometric data derived from our long-slit spectra of HD 44179. We have simply summed along each column to obtain the total flux from the source at each wavelength. The absolute flux levels were obtained by multiplying the reduced data by α Tau's assumed spectrum, a 3800 K Planck blackbody function with a flux of 18.5×10^{-12} W m^{-2} μm^{-1} at 10.00 μm. Because of the narrow (2″) slit used, our data are not truly photometric. From the comparison of spectra obtained of several photometric standards we assign an uncertainty of 15% to the overall level of the spectrum of HD 44179. In Figure 2 we have also plotted the *IRAS* LRS spectrum of HD 44179. Our data lie well below the LRS spectrum. What is particularly striking is the much lower contrast for the spectral features in our data. This is exactly the result we would expect; much of the emission from the spatially resolved features lies outside our slit.

4. DISCUSSION

The results in the previous section clearly demonstrate that at least two regions are producing the 10 μm radiation from HD 44179. One region produces a nearly featureless continuum and is represented by the central source, which we may have marginally resolved. This region corresponds to the 1″.0 $\times$ 0″.4 source and the compact 0″.2 source within it (Dyck et al. 1984; Dainty et al. 1985; Leinert & Haas 1989). The second region is much more extended than the central source and
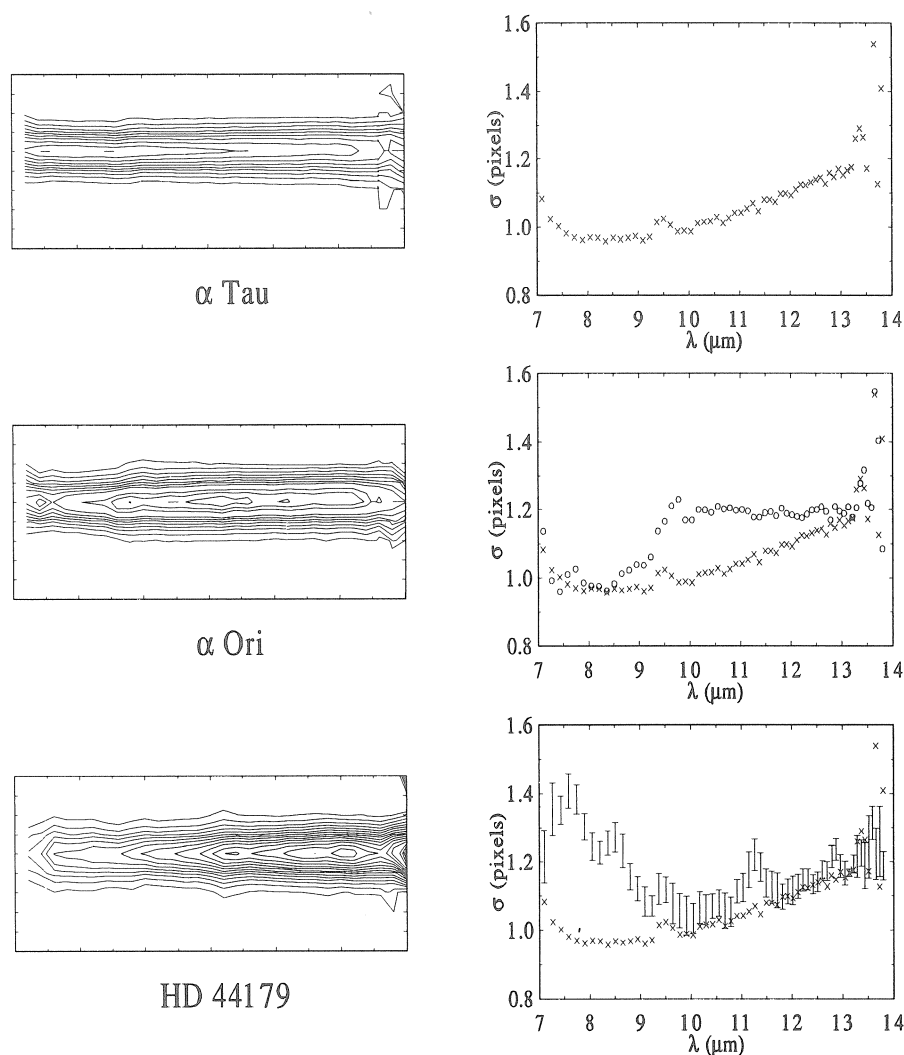
FIG. 1.—Spatial data for (*from top to bottom*) α Tau, α Ori, and HD 44179. On the left are contour plots of the reduced GLADYS images. Each tick on the vertical scale of the contour plot is 1 pixel (0″.9); each tick on the horizontal axis is 5 pixels. Wavelength runs from 7 μm on the left to 14 μm on the right. The spatial extent (vertical axis) of the plots is 9″. Spatiograms of these data are presented on the right. The spatiogram for α Tau is repeated in the lower panels for reference. Each pixel is 0″.88 across. The increase in σ near 9.5 μm is due to the telluric ozone absorption feature.
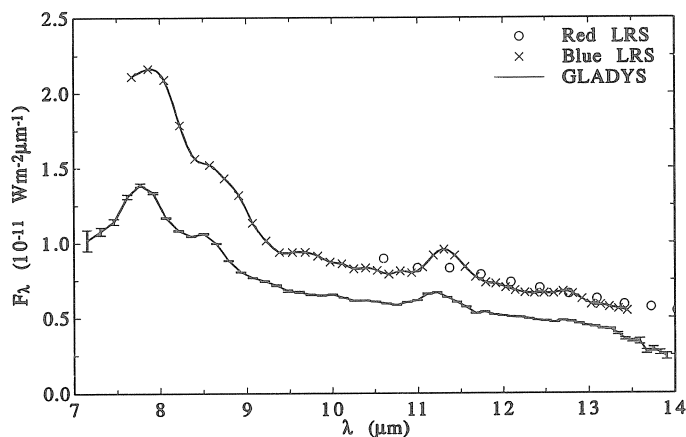

FIG. 2.—The GLADYS spectrum of HD 44179, integrated across the slit. For comparison we have included the LRS spectrum.

produces the UIR features and the 12.8 μm feature. The full extent and exact nature of the extended emission cannot be obtained from the present analysis. The varying contrast between the central source and the extended emission will cause the numerical value of σ to vary from feature to feature even if the extended emission is distributed in precisely the same manner in each spectral feature. Our data do require that the emission features are extended by at least 1″. This conclusion is supported by the detection of 3.3 μm UIR emission 5″ away from the 10 μm source by Geballe et al. (1989).

The central issue in the physical interpretation of our results is what causes the differences in emitted spectra between the two regions. Are they due to differences in the grains, such as their size distribution or chemical composition, or due to differences in the physical conditions in the two zones, such as density or radiation field? The most economical hypothesis at this time is that the grains are the same in both regions, but the fluorescent emission from the smaller grains is swamped in the

GRASDALEN, SLOAN, & LEVAN

inner portions of the nebula by equilibrium emission from the larger grains.

We are presently analyzing similar observations of GL 618 and GL 2688 and will present a more quantitative discussion of all our data in a future paper.

As a technical aside we note that the 12.8 μm feature is not evident in the spectrum of HD 44179 (Fig. 2), whereas its presence is clearly indicated by the spatiogram (Fig. 1). The two-dimensional character of a slit spectrometer is exploited here through a combination of spectral and spatial analysis.

REFERENCES

Bachiller, R., Gómez-González, J., Bujarrabal, V., & Martín-Pintado, J. 1988, A&A, 196, L5
Blanco, A., Bussoletti, E., & Colangeli, L. 1988, ApJ, 334, 875
Cohen, M., et al. 1975, ApJ, 196, 179
Cohen, M., Tielens, A. G. G. M., & Allamandola, L. J. 1985, ApJ, 299, L93
Crampton, D., Crowley, A. P., & Humphreys, R. M. 1975, ApJ, 198, L135
Dainty, J. C., Pipher, J. L., Lacasse, M. G., & Ridgway, S. T. 1985, ApJ, 293, 530
Duley, W. W., & Williams, D. A. 1981, MNRAS, 196, 269
Dyck, H. M., & Benson, J. A. 1991, A Study of the Angular Diameters of Dust Shells around Red Giants, AFOSR-TR-88-0057
Dyck, H. M., Zuckerman, B., Leinert, Ch., & Beckwith, S. 1984, ApJ, 287, 801
Geballe, T. R., Lacy, J. H., Persson, S. E., McGregor, P. J., & Soifer, B. T. 1985, ApJ, 292, 500
Geballe, T. R., Tielens, A. G. G. M., Allamandola, L. J., Moorhouse, A., & Brand, P. W. J. L. 1989, ApJ, 341, 278
Landau, R., Grasdalen, G., & Sloan, G. C. 1992, A&A, in press
Léger, A., & d'Hendecourt, L. 1987, in Polycyclic Aromatic Hydrocarbons and Astrophysics, ed. A. Léger, L. d'Hendecourt, & N. Boccara (Dordrecht: Reidel)
Leinert, Ch., & Haas, M. 1989, A&A, 221, 110
LeVan, P. D. 1990, PASP, 102, 190
Ney, E. P., Merrill, K. M., Becklin, E. E., Neugebauer, G., & Wynn-Williams, C. G. 1975, ApJ, 198, L129
Russell, R. W., Soifer, B. T., & Willner, S. P. 1978, ApJ, 220, 568
Sakata, A., Wada, S., Onaka, T., & Tokunaga, A. T. 1987, ApJ, 320, L63
Sellgren, K. 1990 in Dusty Objects in the Universe, ed. E. Bussoletti & A. A. Vittone (Dordrecht: Kluwer)
Tokunaga, A. T., Nagata, T., Sellgren, K., Smith, R. G., Onaka, T., Nakada, Y., Sakata, A., & Wada, S. 1988, ApJ, 328, 709
Tokunaga, A. T., & Young, E. T. 1980, ApJ, 237, L93
Walker, R., & Price, S. D. 1975, AFCRL Infrared Sky Survey, AFCRL-TR-75-0373
Westbrook, W. E., Becklin, E. E., Merrill, K. M., Neugebauer, G., Schmidt, M., Willner, S. P., & Wynn-Williams, C. G. 1975, ApJ, 202, 407
Witteborn, F. C., Sandford, S. A., Bregman, J. D., Allamandola, L. J., Cohen, M., Wooden, D. H., & Graps, A. L. 1989, ApJ, 341, 270
Zuckerman, B., Gilra, D. P., Turner, B. E., Morris, M., & Palmer, P. 1976, ApJ, 205, L15